Journal of Imaging Science and Technology® 63(6): 060411-1–060411-11, 2019.

Fractional Contrast Stretching for Image Enhancement of Aerial and Satellite Images

Thaweesak Trongtirakul and Werapon Chiracharit
Department of Electronic and Telecommunication, Faculty of Engineering, King Mongkut's University of Technology Thonburi, 126 Pracha Uthit Rd, Bang Mot, Thung Khru, Bangkok, Thailand 10140
E-mail: thaweesak.trongtirakul@mail.kmutt.ac.th

Susan Imberman
Department of Computer Science, College of Staten Island, City University of New York, 2800 Victory Blvd. Staten Island, New York, United States 10314

Sos Agaian
Department of Computer Science, The City University of New York, New York City, New York, United States

Abstract. *Aerial and satellite photographs suffer from uncontrollable weather conditions. Frequently, illumination of the same region can be totally different. This is usually due to shadowing self-obstruction or light reflection. Existing image enhancement methods fail to improve hidden details and local contrast at the same visualization level. They are not developed to enhance through local dark or light regions simultaneously. Also, the current aerial and satellite image enhancement methods have several limitations. For instance, these include intensity saturation, non-uniform brightness, halo effect, blur edges, and so on. This article introduces a fractional contrast stretching concept for aerial and satellite image enhancement based on a novel automated non-uniform luminance normalization that is not provided by the user as input parameters. The introduced approach contains several new techniques: (i) no reference non-linearly fractional contrast stretching with automatic non-uniform luminance normalization and (ii) non-linearly local contrast stretching for spatial details and edge sharpening. The proposed algorithm was tested on the orthorectified aerial photograph database with a pixel resolution of 1 meter or finer from across the United States during 2000–2016. The simulation results illustrate the efficiency of the proposed algorithm and its advantages for cutting-edge aerial and satellite image enhancement, resulting in visualization quality.*

[DOI: 10.2352/J.ImagingSci.Technol.2019.63.6.060411]

1. INTRODUCTION

Remote digitally captured imagery and its various formats try to lay the foundation of the current technology on image enhancement. It is quite absolute that the indispensability of image quality enhancement, recognizable information, and detailed restoration is a primary concern. Since the last decade, satellite remote sensing imagery has been playing an important role in different scientific-based applications in the field of weather, agriculture, aquaculture, resource exploration, etc. Multi-spectral satellite imagery (information within specific wavelength ranges across the electromagnetic spectrum, e.g., Landsat 5, Landsat 7, Landsat 8, WorldView-2, etc.) [1] consisting of high-resolution information (e.g., aerial photographs, panchromatic imagery, etc.) reveals surface geology. Classical explorations are time-consuming and the cost of the investigation in related geological fields is expensive and complex. Modernized remote sensing techniques offer much more efficient and less cost for preliminary geological explorations.

The quality of aerial and satellite photographs before processing is not in good condition for visual interpretation. The poor image quality may come from analog sensing with its corrections in illumination, geological conditions, lens settings, and sensor characteristics. The imagery is still not be optimized for human visualization [2]. In order to enhance poor aerial and satellite photographs, digital image processing allows users to deal with image quality in the pixel-level. Remote sensing devices, especially those managed from satellite platforms, have to be designed to deal with various levels of target illumination/reflection intensities, which are typical for those conditions likely to be found in common use. With large-scale diversification in spectral reflection from various targets, analog corrections cannot optimally account for and display optimal luminance and contrast for all targets. When applying acquired images for different applications, their luminance distributions must be considered.

Contrast stretching (CS) and enhancement are regularly offered to be an important method of digital image processing, used to highlight features in an input image. There are several traditional techniques (global histogram equalization (GHE), local histogram equalization (LHE), linear and non-linear CS families) and existing image enhancement techniques [3–8]. Those enhancement techniques occasionally generate side effects such as over-enhancement, washed-out details, noise magnifications, and several artifacts. To resolve those issues, GHE frequently generates over-enhancement and over-brightness. LHE sometimes produces unpleasant details and blocking effects in a compressed image. However,

Received July 13, 2019; accepted for publication Oct. 19, 2019; published online Jan. 7, 2020. Associate Editor: Steven Simske.
1062-3701/2019/63(6)/060411/11/$25.00

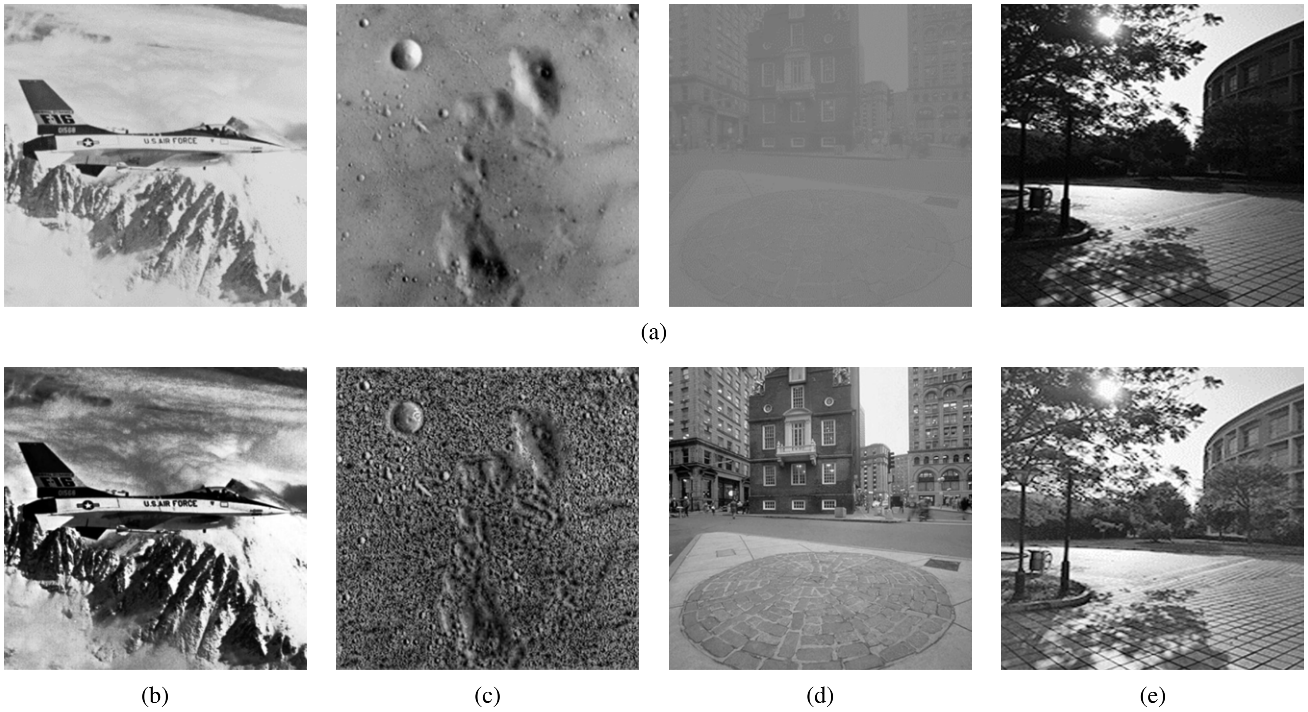

Figure 1. Comparison of existing classical contrast enhancements and contrast stretching techniques. (a) Original image; (b) GHEed image; (c) LHEed image; (d) linear stretched image; (e) piecewise non-linear stretched image.

CS families are the simplest tool for organizing luminance and slightly increasing contrast. CS can be classified into two large-scale methods: (i) the global CS method is beneficial for low contrast images and can preserve luminance in the case where the original distribution is almost fully distributed; (ii) the piecewise CS method considers the distribution of luminance in a specific range and can be applied to non-uniform luminance applications such as backlit images and underwater images including hazy images (see Figure 1). The contrast stretching classes of aerial and satellite photograph enhancements can be classified into two classes: classical contrast stretching class and implemented contrast stretching class.

1.1 *Classical Contrast Stretching Class*

An important first step is to initially normalize the luminance in an image. This increases the accuracy of brightness-based features which helps in computer-aided detection systems. This section will give a brief overview of classical contrast stretching classes in terms of their advantages, limitation, and applications. Linear contrast stretching classes arrange luminance distribution into a low dynamic range. They try to efficiently improve low contrast images. If the considered images are fully distributed (95%–100% distribution) in a permitted range, the luminance results are slightly improved or preserved. To enhance the contrast and brightness (visibility) of interested regions, the luminance distribution can be considered by a specific low dynamic range (LDR) and performed on a high dynamic range (HDR) [9, 10]. Due to the limitation of the high dynamic distribution, unconsidered LDRs are automatically condensed by expanding the luminance on HDR. The non-linear contrast stretching classes attempt to generate high contrast by unevenly shifting luminance levels [9] and organizing brightness at the same time. Although these methods are very powerful for improving visualization, over-enhancement, over-brightness, and wash-out effects are among frequently occurring side effects. Piecewise non-linear contrast stretching is one of the smart methods to handle these limitations [11]. However, optimal non-linear parameters are used to avoid undesired artifacts and present the best image quality [12–19] (see Table I).

1.2 *Implemented Contrast Stretching Class*

In the last decade, Tarel et al. [20] introduced fast visibility restoration from a single color or gray level image for surveillance, intelligent vehicles, and remote sensing systems. His approach has complexity of a linear function of a number of input image pixels. The primary problem with this method is that it does not perform well when the image's appearance is occluded by weather conditions such as haze and fog or environmental factors such as smoke. The algorithm strives to remove hazy effects. Thus, hazy regions become darker regions. As a result of configuring highly restored visibility parameters, colors in the enhanced image may appear over-saturated and extremely dark.

Table I. Cutting-edge image enhancement of satellite and aerial photographs.

Method / Applications	Key Solutions	Description
Method: Linear contrast stretching **Applications:** Low contrast images, luminance-scaling based applications	$Y_{i,j} = (X_{i,j} - X_{min})\left(\frac{Y_{max}-Y_{min}}{X_{max}-X_{min}}\right) + Y_{min}$	X_{max} and X_{min} are the maximum and minimum intensity of an input image. Y_{max} and Y_{min} are the maximum and minimum intensity of an output image
Method: Piecewise linear contrast stretching [3] **Applications:** Low contrast images	$Y_{i,j} = \begin{cases} 0, & X_{i,j} \le X_{min} \\ \frac{k(X_{i,j}-X_{min})}{b-X_{min}}, & X_{min} < X_{i,j} < b \\ k + \frac{(1-k)(X_{i,j}-b)}{X_{max}-b}, & b < X_{i,j} < X_{max} \\ 1, & X_{i,j} \ge X_{min} \end{cases}$	k is taken equal to the value from the interval of $k \in [(1-\mu)b, \mu + (1-\mu)b]$ μ limits the range of possible value for k. b is the average value of the brightness.
Method: Partial contrast stretching [4] **Applications:** Acute Leukemia	$Y_{i,j} = \begin{cases} \frac{Y_{min}X_{i,j}}{T_{min}}, & X_{i,j} \le T_{min} \\ \left(\frac{Y_{max}-Y_{min}}{T_{max}-T_{min}}\right)(X_{i,j} - T_{min}) + Y_{min}, & T_{min} < X_{i,j} < T_{max} \\ \left(\frac{X_{i,j}-T_{max}}{255-T_{max}}\right)(255 - Y_{max}) + Y_{max}, & X_{i,j} \ge T_{max} \end{cases}$	$T_{max} = \frac{1}{3}\max_{k=1,2,3}(X_{i,j,k})$ $T_{min} = \frac{1}{3}\min_{k=1,2,3}(X_{i,j,k})$
Non-linear contrast stretching [3]	$Y_{i,j} = \left(\frac{1}{1+e^{-a(X_{i,j}-b)}}\right)\left(\frac{Y_{max}-Y_{min}}{X_{max}-X_{min}}\right) + Y_{min}$ $Y_{i,j} = (Y_{max} - Y_{min})\left(\frac{X_{i,j}-X_{min}}{X_{max}-X_{min}}\right)^{\gamma} + Y_{min}$ $Y_{i,j} = (Y_{max} - Y_{min})\int_0^{X_{L-1}} p(X_{i,j}) + Y_{min}$	a is a contrast parameter. b is a brightness parameter. γ is a gamma parameter $p(\cdot)$ is a statistical function. L is the total level of a permitted range.
Method: Piecewise non-linear contrast stretching [5] **Application:** Brightness and contrast enhancement	$Y_{i,j} = \begin{cases} g(1 + X_{i,j})^{q}, & X_{i,j} \le 80 \\ aX_{i,j} + b, & X_{i,j} > 80 \end{cases}$	$a = 0.17, b = 211.3, g = 25$ and $q = 0.5$.
Applications: Luminance adaptation projection in a just-different noticeable (JND) [6-10, 30-34]	$Y_{i,j} = \begin{cases} 17\left(1 - \sqrt{\frac{X_{i,j}}{t}}\right), & X_{i,j} \le t \\ \frac{3}{128}(X_{i,j} - t) + 3, & X_{i,j} > t \end{cases}$	t is a middle luminance level of $X_{i,j}$.

Recently, Jadhav et al. [21] focused on satellite image enhancement based on interpolation of the high-frequency sub-bands obtained by discrete wavelet transform and a low-resolution input image. The limitation of LANDSAT8™ multi-spectral sensor is that it provides a total of 11 banks of data with a 30-square-meter resolution. That image resolution is not sufficient for specific applications. The algorithm uses a bilinear interpolation by a factor of two for upscaling the original resolution on wavelet sub-bands. The resulting images are quite dark, lack contrast, and suffer from blocking effects due to wavelet composition.

Daway et al. [22] implemented the fast visibility restoration algorithm for aerial image enhancement based on a sigmoid function. The main focus of this method is to attempt to normalize a luminance distribution using a non-linear function before applying image enhancement. Their implementation improves luminance and contrast in aerial images with poor visibility and provides a better visual representation and edge information. However, it generates artificial colors in over-exposed regions.

Last year, Chandra et al. [23] presented an effective method for improving the contrast of hazed aerial images by computing its dark channel image, calculating the atmospheric luminance, recovering the scene radiance, and refining enhanced details by gamma correction. Their resulting images are effectively de-hazed, and contrast is improved with a high structural similarity value. The drawback of this approach is that the results become darker.

Although these methods are attractive, classes of methods suffer from well-known weaknesses in equalization methods: some regions become over-enhanced, have increased brightness saturation, and are unnatural looking. Also, they suffer from increases in blocking effects, the halo effect, and noise. Contrast stretching families perform well on low contrast images and non-uniform luminance images by addressing luminance distribution, but stretched results lack contrast. These cutting-edge image enhancement methods for aerial and satellite photographs (see Table II) attempt to incorporate the advantages inherent in contrast stretching concepts. Notwithstanding, they also generate various undesirable artifacts. Commonly used remote sensing applications of various image contrast stretching methods have been implemented over the last decades. These classical stretching functions have various limitations and challenges. There currently exists no research on using a fractional contrast stretching function to resolve such issues.

Table II. Cutting-edge image enhancement of satellite and aerial photographs.

Method / Applications	Key Solutions	Description
Method: Fast visibility restoration [20] (2009) **Applications:** Surveillance, intelligent vehicles, and remote sensing systems	$R_{i,j} = \frac{I_{i,j} - V_{i,j}}{1 - \frac{V_{i,j}}{I_s}}$; $I_s = 1$ $V_{i,j} = max\left(min\left(pB_{i,j}, W_{i,j}, 0\right)\right)$; $p = 0.95$ $B_{i,j} = A_{i,j} - med\lvert W - A\rvert_{i,j}^{m,n}$ $A_{i,j} = med[W]_{i,j}^{m,n}; m, n = 41, 41$	$I_{i,j}$ is an input image. $W_{i,j} = \begin{cases} I_{i,j}, & gray \\ \min\limits_k\left(I_{i,j,k}\right), & color \end{cases}$
An effective method for satellite image enhancement [21] (2015) **Applications:** Low-resolution satellite image (LANDSAT8 TM)	$J_{i+m,j+n,k} = (1-\alpha)D_{i,j} + \alpha\psi_{i+m,j+n,k}$	$D_{i,j}$ is a subtracted image. $\psi_{i,j,k}$ is a wavelet component. α is a weight, $0 \leq \alpha \leq 1$.
Aerial image enhancement using modified fast visibility restoration based on sigmoid function [22] (2016) **Applications:** Low contrast aerial images, under-water images with poor visibility	$Y_{i,j} = \frac{1}{1 + \left[\frac{(1-a)\left(1 - I_{i,j}\right)}{aI_{i,j}}\right]^{0.8}}$	$I_{i,j}$ is an input luminance. a is a contrast parameter.
De-hazing of aerial images by dark channel and gamma correction [23] (2018) **Applications:** Geoscience aerial image with poor weather conditions. Mapping lithology, vegetation coverage, and mineral exploration.	$PL_{i,j} = 255\left(L_{i,j}\right)^{1/\gamma}$; $\gamma = 1.5$ $J_{i,j,k} = \frac{I_{i,j,k} - A}{max\left(T_{i,j}, T_0\right)} + A$ $T_{i,j} = 1 - \min\limits_k I_{i,j,k}$ $A = arg\max\left(\min\limits_k I_{i,j,k}\right)$	$L_{i,j}$ is the luminance of a de-hazed image $\left(J_{i,j,k}\right)$. $T_{i,j}$ is the transmission map of a hazy image. $I_{i,j,k}$ is a hazy aerial image. γ is gamma correction.

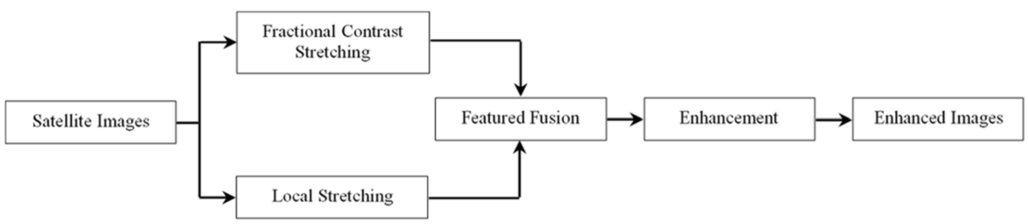

Figure 2. The framework of our fractional contrast stretching for the image enhancement of aerial and satellite photographs.

Consequently, the non-linearly fractional contrast stretching advancements in image processing applications are still an open research area.

In this article, we address the above-stated problems. The rest of the article is organized as follows: Section 2 presents a new fractional contrast stretching concept for image enhancement of aerial and satellite photographs. Section 3 presents a computer simulation and illustrates the performance of the proposed method along with the results. Section 4 offers our conclusions.

2. PROPOSED METHOD

In this section, we present a fractional contrast stretching concept for the image enhancement of aerial and satellite photographs through a luminance domain. The proposed concept consists of four main steps (see Figure 2).

2.1 *Fractional Contrast Stretching*

In general, most aerial and satellite photographs have a different average brightness. The application of image enhancement methods without a luminance normalization process results in unwanted artifacts. Therefore, the proposed luminance normalization is carried out by non-linearly fractional stretching functions applied to its brightness scale, at which the average luminance of the transformed image is close to the middle permitted range.

$$FCS_{i,j} = FCS_{\max}\left(\frac{\bar{S}_{i,j} - \bar{S}_{\min}}{FCS_{\max} - FCS_{\min}}\right) + FCS_{\min} \qquad (1)$$

$$\bar{S}_{i,j} = \begin{cases} \dfrac{S_{i,j} - S_{\min}}{\lvert S_{\min}\rvert + S_{\max}}, & S_{\min} < 0 \\ S_{i,j}, & S_{\min} \geq 0 \end{cases} \qquad (2)$$

$$S_{i,j} = \frac{1}{N}\sum_{k=1}^{N} \omega_k \diamond \left(\frac{I_{i,j} - I_{\min}}{I_{\max} - I_{\min}}\right)^{\gamma_k} \qquad (3)$$

$$\gamma_k = \begin{cases} \{0.1 \le \gamma \le 1.0\}, & \mu_I \le \dfrac{L-1}{2} \\ \{1.0 \le \gamma \le 2.0\}, & \mu_I > \dfrac{L-1}{2}, \end{cases} \tag{4}$$

where $\diamond$ is a fractional weighing operator (a fractional weighing operator can be set as a dot operator and the condition can be written as $\omega_k \le 1, \sum_{k=1}^{N} \omega_k = 1$). $I_{i,j}$ is a considered image. $()_{\min}$ and $()_{\max}$ are, respectively, the minimum and maximum luminance of the function in a bracket. L and μ_I are the total luminance level in the permitted range and the mean brightness of $I_{i,j}$.

2.2 *Local Contrast Stretching*

A local contrast stretching (LCS) method performs on a low dynamic range and maps the considered intensities onto a high dynamic range. LCS locally performs on a luminance domain by adjusting each pixel intensity to improve the thin edges and finely detailed visualization of regions in both dark and light components simultaneously. LCS operates on the visualization by sliding blocks (kernels) over the considered image and modifying the center pixel intensity.

$$LCS_{i,j} = (L-1)\left(\frac{I_{i,j} - [I_{\min}]_{i,j}^{m,n}}{[I_{\max}]_{i,j}^{m,n} - [I_{\min}]_{i,j}^{m,n}}\right)^{\delta_{i,j}}, \tag{5}$$

where $I_{i,j}$ is a considered image; $I_{\min}$ and $I_{\max}$ are the minimum and maximum luminance of $I_{i,j}$; L is the total luminance level in the high dynamic range; m, n is the size of a sliding block; and $\delta_{i,j}$ is an exponential weighting metric.

2.3 *Contrast Stretching Fusion*

A contrast stretching fusion method attempts to fuse several distinguished features into the same visualization. Also, the fusion function enables us to adjust the best outstanding feature by using a weighting fusion.

$$F_{i,j} = \alpha FCS_{i,j} + (\alpha - 1)\, LCS_{i,j};\ 0 \le \alpha \le 1, \tag{6}$$

where $FCS_{i,j}$ is a fractional contrast stretched image; LCS is a local stretched image; and α is a weight.

3. COMPUTER SIMULATION

Our computer simulation tests orthorectified aerial photographs with a pixel resolution of 1 meter or finer from across the United States during 2000–2016 [24]. Experimental computer simulation results with comparative performance and evaluation are done by a reimplementation of various state-of-the-art methods.

3.1 *Contrast Stretching Function for Normal Luminance Distribution*

We experiment with the performance of the proposed stretching algorithm in the orthorectified aerial photographs. In Figure 3, we make a comparison with aerial and satellite images that are computed by the proposed non-linearly fractional stretching functions with various cutting-edge stretching algorithms. It is evident that the new non-linearly fractional stretching functions, by a spatial pixel-based intensity method, achieve a uniform brightness with all parts of the image suitably projected, leading to superior details. The other existing resulting images lose some significant details (see Fig. 3(d)) and luminance details (see Fig. 3(f)). The rest cannot normalize overall luminance brightness into the normal distribution. Before applying any image enhancement algorithms, the normalization of the luminance distribution process is very important because (1) if dark parts are enhanced, the enhanced regions will be darker. Occasionally, it is very difficult to recognize what details are present. (2) If bright parts are enhanced, the enhanced regions will become over-enhanced. Hence, significant information might be lost by intensity saturation.

3.2 *Contrast Enhancement for Aerial Photographs*

We tested the proposed satellite image enhancement method on several aerial and satellite photographs. In this experiment, we present our enhanced results and make a comparison with existing satellite image enhancement [20–23] and traditional contrast enhancement methods.

As the results in Figure 4, the proposed images along with the existed enhancement approaches the in-depth detailed investigation. The traditional image enhancement techniques (histogram equalization: HE (Fig. 4(b)) and bi-brightness histogram equalization: BBHE (Fig. 4(c))) commonly tend to generate intensity saturation on both dark and bright components. Meanwhile, the state-of-the-art enhancement techniques (Chandra's method [23] (Fig. 4(d)), Jadhav's method [21] (Fig. 4(e)), Tarel's method [20] (Fig. 4(f)), and Daway's method [22] (Fig. 4(g))) attempt to avoid the such unpleasant effects, but still some parts of dark components remain in the enhanced images. The proposed enhancement technique achieves the best image enhancement in an adaptive manner on both dark and bright components. The first row and the fourth row of Fig. 4(h) illustrate more details in the dark components (the red square) by reducing an intensity saturation. In addition, the third row of Fig. 4(h) presents more details and sharp edges.

In order to prove the visual quality of the proposed technique, Figure 5 (the red squares are extracted from Fig. 4) illustrates the challenged regions. They highlight excellent perceptual image quality in terms of sharpness, edges boundaries, contrast, and luminance features and also tend to enhance adaptively the luminance without introducing unwanted effects.

4. CONCLUSION

We present a novel non-linearly fractional contrast stretching method for aerial and satellite photographic enhancement, with spatially automatic luminance normalization for contrast enhancement. The proposed method: (1) normalizes global luminance (pre-enhancement) by shifting estimated luminance to the middle scale of a permitted range; (2) produces a sharp edge feature (feature enhancement) by generating local linear stretching functions; and (3) enhances normalized luminance image by applying a multiscale

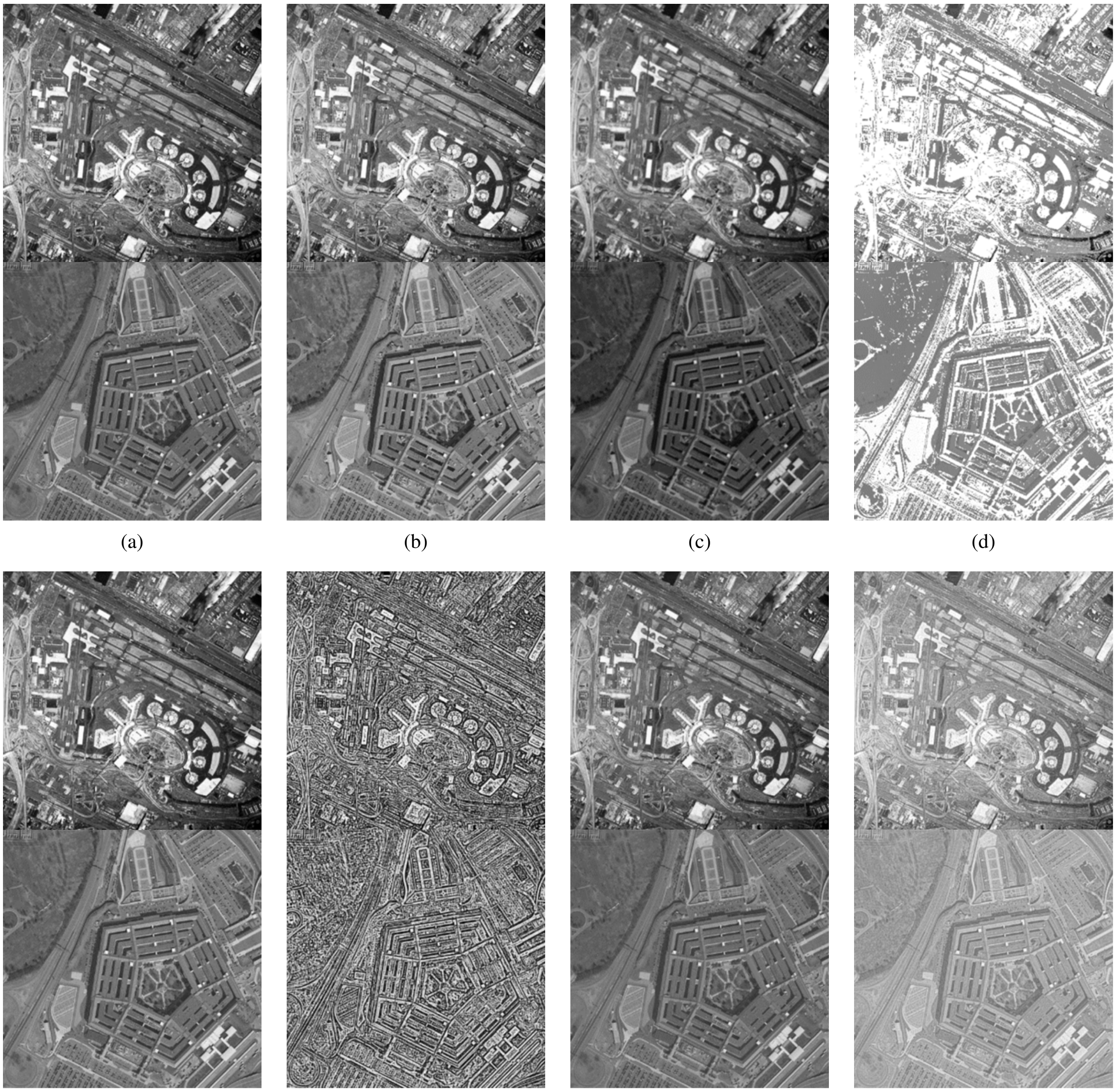

(a) (b) (c) (d) (e) (f) (g) (h)

Figure 3. Stretched images. (a) Original image; (b) Sergei's image [25]; (c) Murinto's image [26]; (d) piecewise non-linear stretched image [27]; (e) linear stretched image; (f) local linear stretched image [28]; (g) sigmoid stretched image [29]; (h) non-linearly fractional stretched image.

Retinex algorithm. Empirical results are presented to exhibit the efficacy of the proposed method.

Moreover, the proposed method is a spatial-based image enhancement and a simple method to implement for image enhancement of aerial and satellite photographs. It can be applied to the image fusion and reconstruction of panchromatic and multi-spatial images.

ACKNOWLEDGMENT

Special thanks to the National Science and Technology Development Agency (NSTDA) for the educational sponsorship grant. This work was partially supported by facilities grants to access the facilities in the Computer Science Department, College of Staten Island (CSI), City University of New York (CUNY).

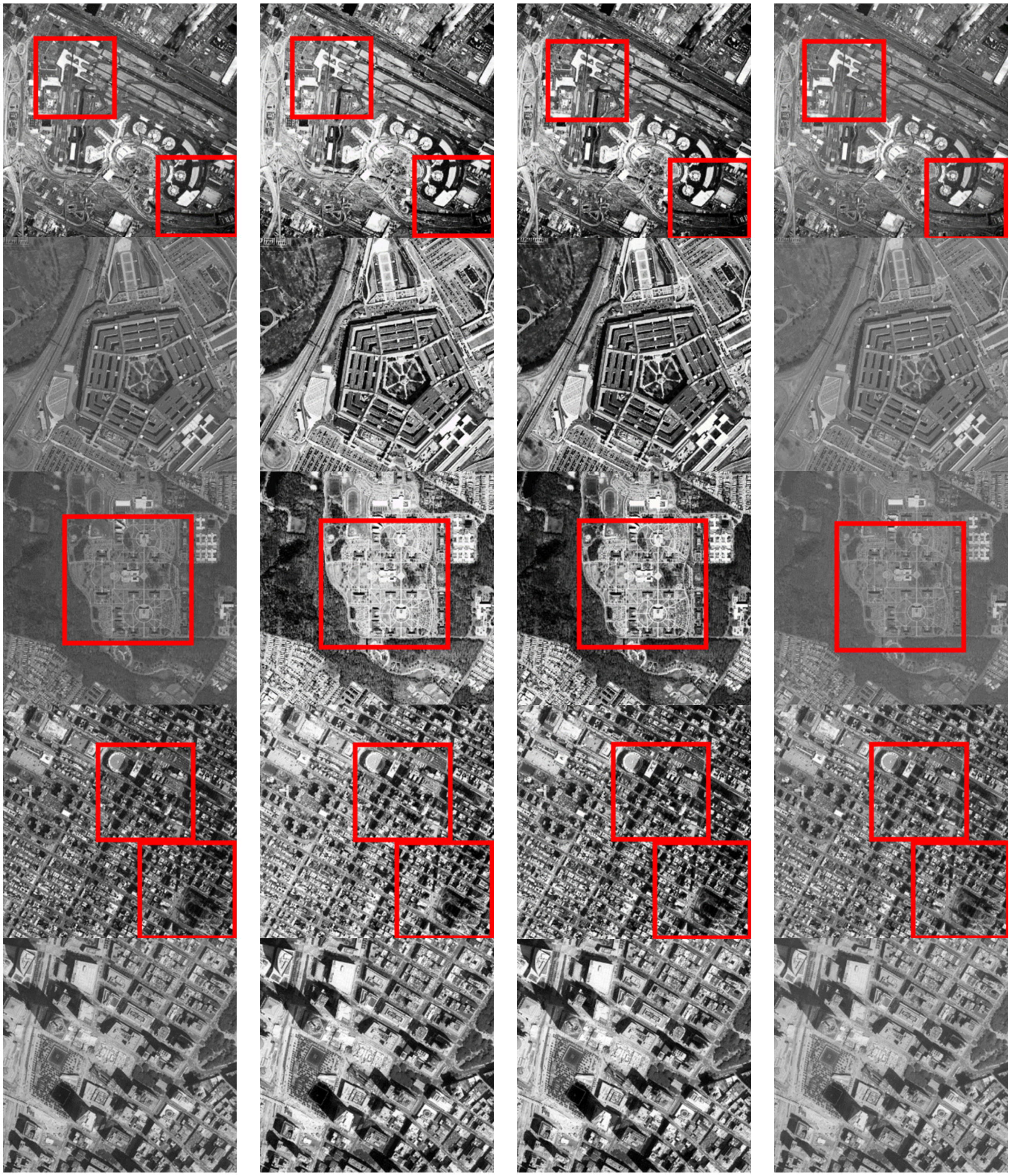

(a) (b) (c) (d)

Figure 4. Continued on next page.

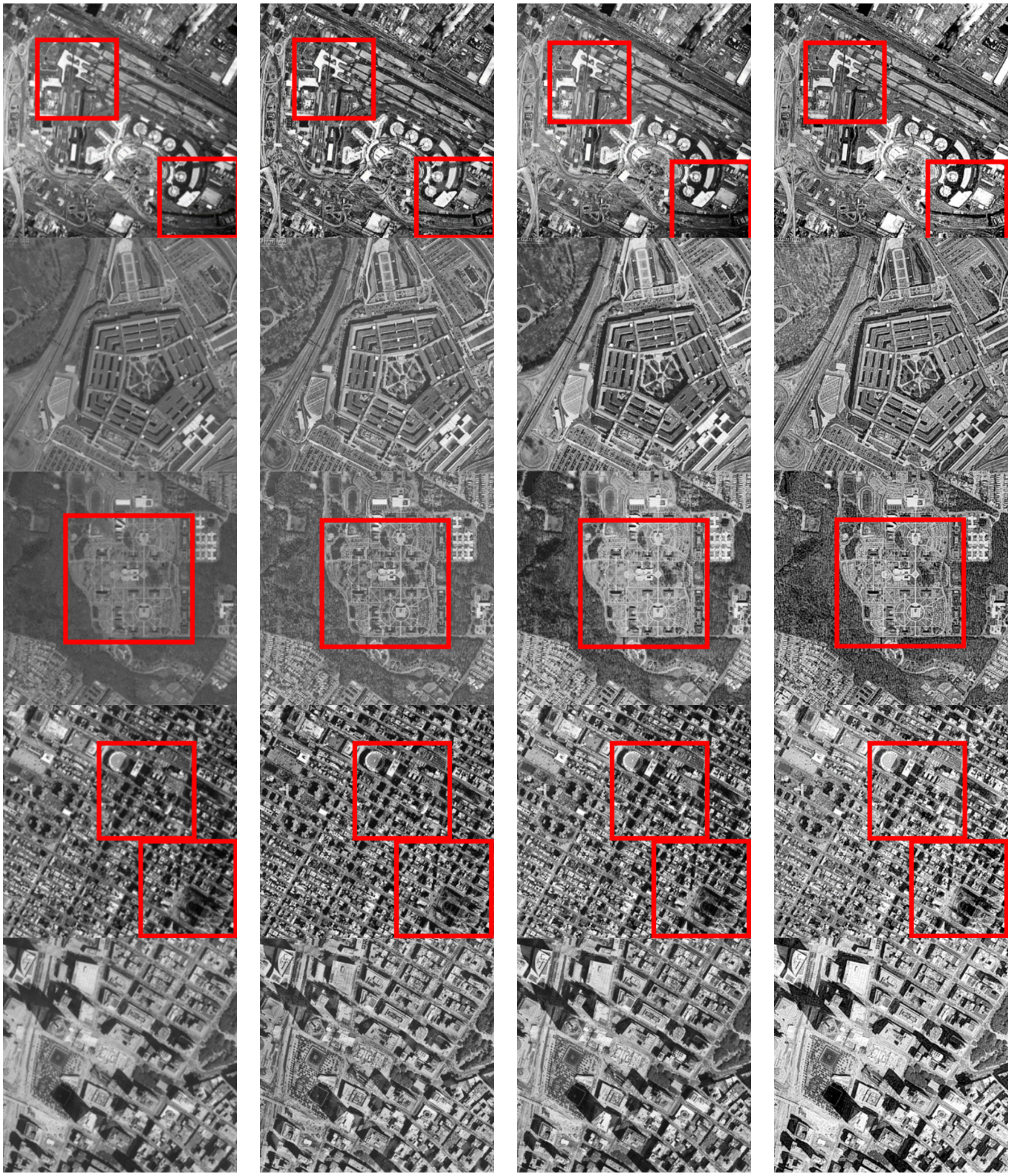

(e) (f) (g) (h)

Figure 4. Enhanced images. (a) Original image; (b) HE's method; (c) BBHE's method; (d) Chandra's method [23]; (e) Jadhav's method [21]; (f) Tarel's method [20]; (g) Daway's method [22]; (h) proposed image.

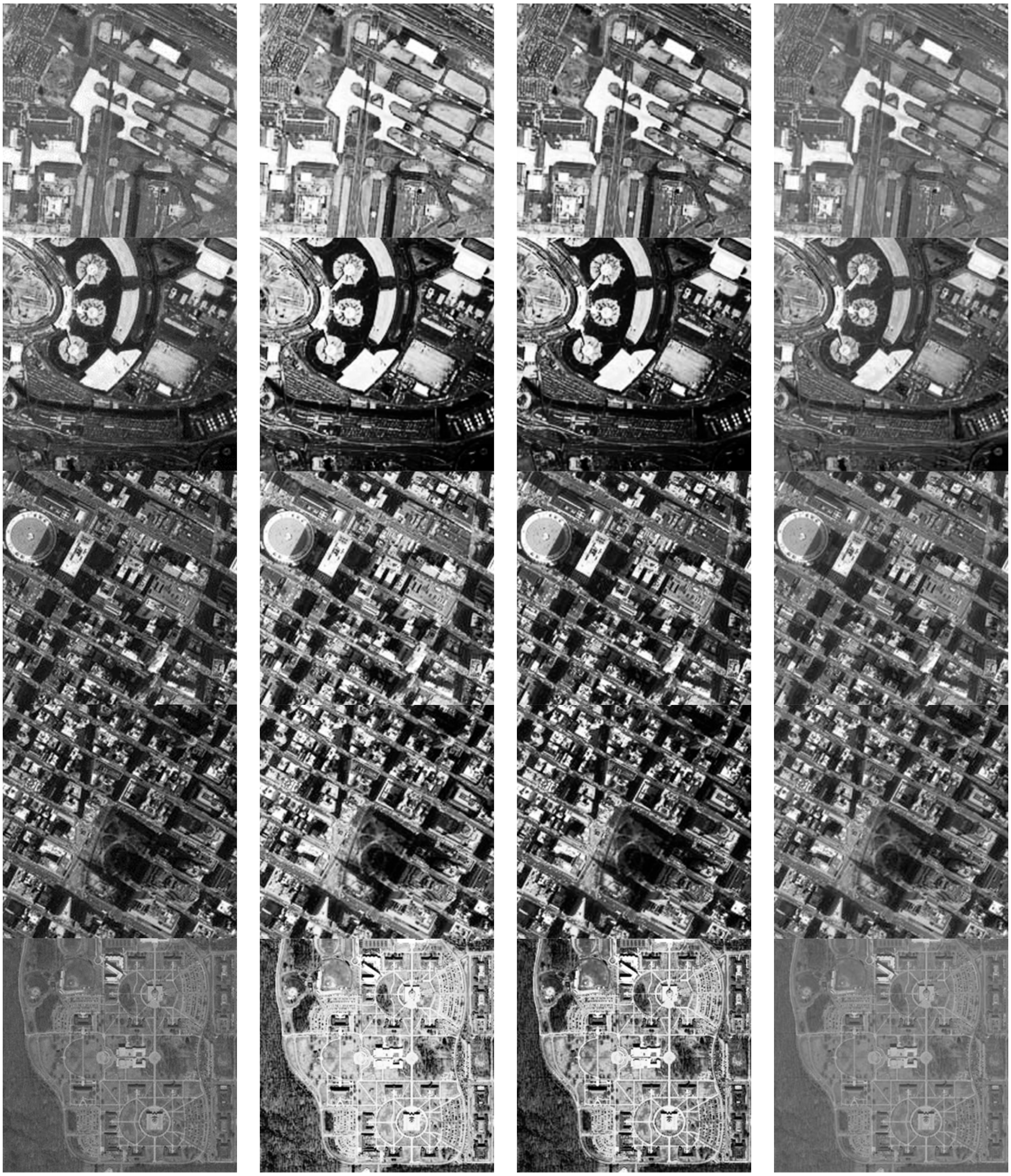

(a) (b) (c) (d)

Figure 5. Continued on next page.

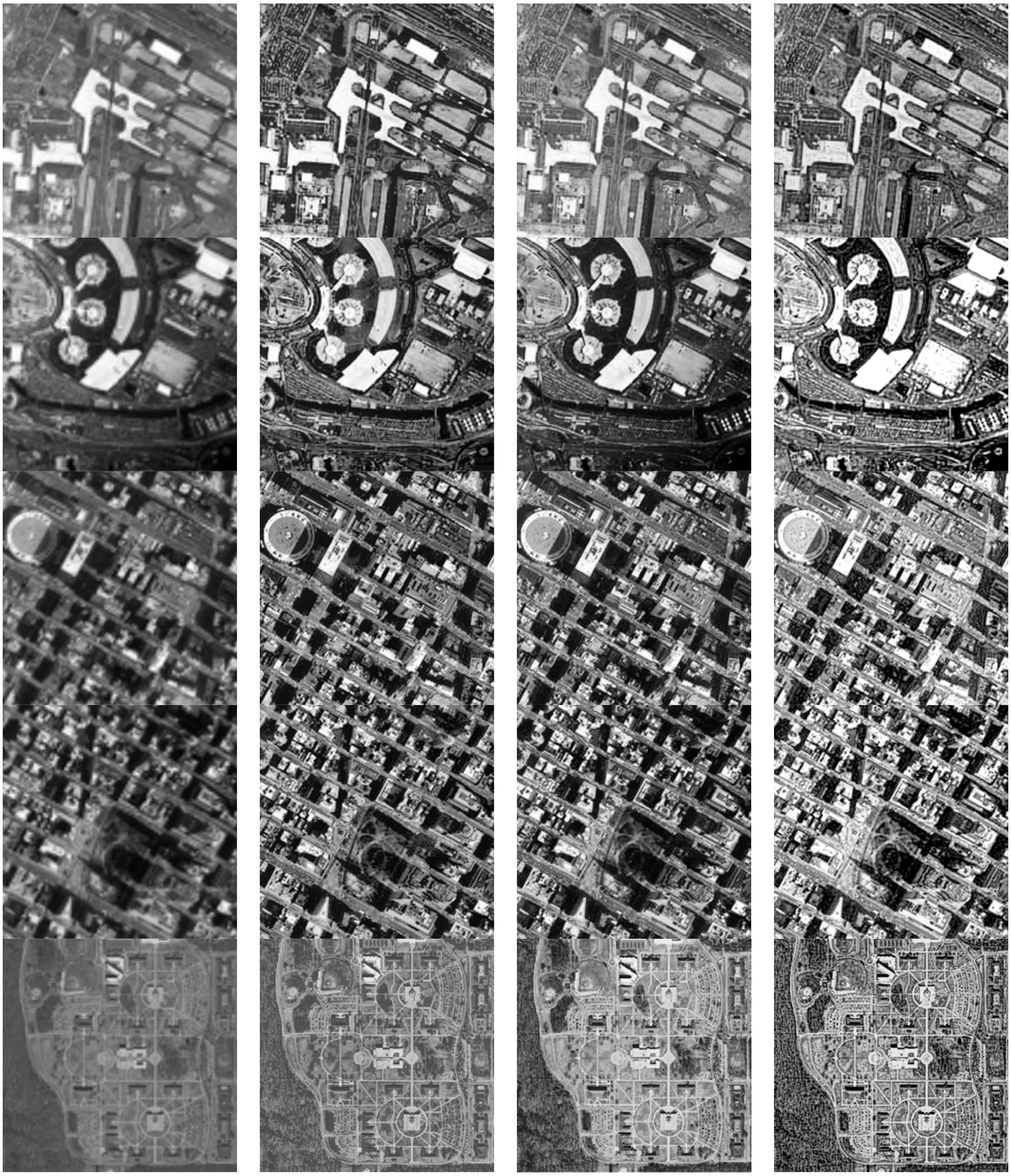

(e) (f) (g) (h)

Figure 5. Extracted images of Fig. 4. (a) Original image; (b) HE's method; (c) BBHE's method; (d) Chandra's method [23]; (e) Jadhav's method [21]; (f) Tarel's method [20]; (g) Daway's method [22]; (h) proposed image.

REFERENCES

[1] O. Kenji, T. Corpetti, and L. Demagistri, "Multispectral satellite image processing," *Optical Remote Sensing of Land Surface* (Elsevier, Amsterdam, the Netherlands, 2016), pp. 57–124.

[2] S. Ahuja and B. Seema, "A survey of satellite image enhancement techniques," Int. J. Adv. Innovative Res. **2**, 131–136 (2018).

[3] S. S. Agaian, K. Panetta, and A. M. Grigoryan, "Transform-based image enhancement algorithms with performance measure," IEEE Trans. Image Process. **10**, 367–382 (2001).

[4] S. S. Agaian, B. Silver, and K. A. Panetta, "Transform coefficient histogram-based image enhancement algorithms using contrast entropy," IEEE Trans. Image Process. **16**, 741–758 (2007).

[5] A. Samani, K. Panetta, and S. Agaian, "Transform domain measure of enhancement–TDME–For security imaging applications," *Proc. IEEE Int'l. Conf. Technol. Homeland Security (HST)* (IEEE, Piscataway, NJ, 2013), pp. 265–270.

[6] K. Panetta, A. Samani, and S. Agaian, "Choosing the optimal spatial domain measure of enhancement for mammogram images," Int. J. Biomed. Imaging **2014**, 937849 (2014).

[7] K. A. Panetta, E. J. Wharton, and S. S. Agaian, "Human visual system based image enhancement and logarithmic contrast measure," IEEE Trans. Syst. Man Cybern. B **38**, 174–188 (2008).

[8] B. Silver, S. Agaian, and K. Panetta, "Contrast entropy-based image enhancement and logarithmic transform coefficient histogram shifting," *Proc. IEEE Int'l. Conf. Acoust. Speech, Signal Process.* (IEEE, Piscataway, NJ, 2005), pp. 633–636.

[9] S. Yelmanov and Y. Romanyshyn, "Image enhancement in automatic mode by piecewise nonlinear contrast stretching," *2018 IEEE First International Conference on System Analysis & Intelligent Computing (SAIC)* (IEEE, Piscataway, NJ, 2018), pp. 1–6.

[10] L. B. Toh, M. Y. Mashor, P. Ehkan, H. Rosline, A. K. Junoh, and N. H. Harun, "Implementation of high dynamic range rendering on acute leukemia slide images using contrast stretching," *2016 3rd Int'l. Conf. on Electronic Design (ICED)* (IEEE, Piscataway, NJ, 2016), pp. 491–496.

[11] X. Yang and X. Lin, "Brightening and denoising lowlight images," *2015 10th Int'l. Conf. on Information, Communications and Signal Processing (ICICS)* (IEEE, Piscataway, NJ, 2015), pp. 1–5.

[12] H. Wang, "VideoSet: A large-scale compressed video quality dataset based on JND measurement," J. Vis. Commun. Image Represent. **46**, 292–302 (2017).

[13] X. Yang, W. Lin, Z. Lu, E. Ong, and S. Yao, "Motion-compensated residue preprocessing in video coding based on just-noticeable-distortion profile," *IEEE Trans. Circuits Syst. Video Technol.* (IEEE, Piscataway, NJ, 2005), pp. 742–752.

[14] C.-H. Chou and Y.-C. Li, "A perceptually tuned subband image coder based on the measure of just-noticeable-distortion profile," IEEE Trans. Circuits Syst. Video Technol. **5**, 467–476 (1995).

[15] Z. Wei and K. N. Ngan, "Spatio-Temporal Just Noticeable Distortion Profile for Grey Scale Image/Video in DCT Domain," IEEE Trans. Circuits Syst. Video Technol. **19**, 337–346 (2009).

[16] X. H. Zhang, W. S. Lin, and P. Xue, "A new DCT-based just-noticeable distortion estimator for images," *Fourth Int'l. Conf. on Information, Communications and Signal Processing, 2003 and the Fourth Pacific Rim Conference on Multimedia. Proceedings of the 2003 Joint* (IEEE, Piscataway, NJ, 2003), pp. 287–291.

[17] A. Samani, K. Panetta, and S. Agaian, "TDMEC, a new measure for evaluating the image quality of color images acquired in vision systems," *Proc. IEEE Int'l. Conf. Technol. Practical Robot Appl.* (IEEE, Piscataway, NJ, 2015), pp. 1–5.

[18] A. Samani, K. Panetta, and S. Agaian, "Quality assessment of color images affected by transmission error, quantization noise, and noneccentricity pattern noise," *Proc. IEEE Int'l. Symp. Technol. Homeland Security (HST)* (IEEE, Piscataway, NJ, 2015), pp. 1–6.

[19] E. A. Silva, K. Panetta, and S. S. Agaian, "Quantifying image similarity using measure of enhancement by entropy," Proc. SPIE **6579** (2007).

[20] J. Tarel and N. Hautière, "Fast visibility restoration from a single color or gray level image," *2009 IEEE 12th Int'l. Conf. on Computer Vision* (IEEE, Piscataway, NJ, 2009), pp. 2201–2208.

[21] B. D. Jadhav and P. M. Patil, "An effective method for satellite image enhancement," *Int'l. Conf. on Computing, Communication & Automation* (IEEE, Piscataway, NJ, 2015), pp. 1171–1175.

[22] H. G. Daway, F. S. Mohammed, and D. A. Abdulabbas, "Aerial image enhancement using modified fast visibility restoration based on sigmoid function," Adv. Nat. Appl. Sci. **10**, 16–22 (2016).

[23] A. Chandra, A. Singh, R. Kumar, and N. Dey, "Dehazing of aerial images by dark channel and gamma correction," *2018 3rd Int'l. Conf. and Workshops on Recent Advances and Innovations in Engineering (ICRAIE)* (IEEE, Piscawatay, NJ, 2018), pp. 1–7.

[24] USGS Database website, https://earthexplorer.usgs.gov, accessed July 2019.

[25] S. Yelmanov and Y. Romanyshyn, "Image contrast enhancement in automatic mode by nonlinear stretching," *2018 XIV-th Int'l. Conf. on Perspective Technologies and Methods in MEMS Design (MEMSTECH)* (2018), pp. 104–108.

[26] S. W. Murinto, D. P. Ismi, and A. Prahara, "Image enhancement using piecewise linear contrast stretch methods based on unsharp masking algorithms for leather image processing," *2017 3rd Int'l. Conf. on Science in Information Technology (ICSITech)* (IEEE, Piscataway, NJ, 2017), pp. 669–673.

[27] T. Trongtirakul, D. Ladyzhensky, W. Chiracharit, and S. Agaian, "Non-linear contrast stretching with optimizations," Proc. SPIE **10993**, 1099303 (2019).

[28] N. Radha and M. Tech, "Comparison of contrast stretching methods of image enhancement techniques for acute leukemia images," Intl. J. Eng. Res. Technol. **1** (2012).

[29] H. G. Daway, F. S. Mohammed, and D. A. Abdulabbas, "Aerial image enhancement using modified fast visibility restoration based on sigmoid function," Adv. Nat. Appl. Sci. **10**, 16–22 (2016).

[30] S. Xu, M. Yu, G. Jiang, and S. Fang, "New just noticeable coding distortion model for perceptual coding," *2016 Digital Media Industry & Academic Forum (DMIAF)* (IEEE, Piscataway, NJ, 2016), pp. 180–184.

[31] Y. Bai, Y. Zhang, and Z. Li, "3D video coding using just noticeable depth difference based on H.265/HEVC," *2015 11th Int'l. Conf. on Computational Intelligence and Security (CIS)* (IEEE, Piscataway, NJ, 2015), pp. 142–145.

[32] X. Qiang, Z. Qiyan, L. Ming Ronnier, G. Haiting, and S. Dragan, "A study of visible chromatic contrast threshold based on different color directions and spatial frequencies," *Proc. IS&T CIC26: Twenty-Sixth Color and Imaging Conference* (IS&T, Springfield, 2018), pp. 53–58.

[33] K. Minsub, S. Ki Sun, and K. Moon Gi, "No-reference image contrast assessment based on just-noticeable-difference," *IS&T Electronic Imaging: Image Quality and System Performance Proceedings* (IS&T, Springfield, VA, 2017), pp. 26–29.

[34] H. Rafael, T. Alain, M. Manuel, G.-R. Luis, C. Guihua, and L. Ronnier, "Checking recent colour-difference formulas with a dataset of metallic samples and just noticeable colour-difference assessments," *IS&T Conf. on Colour in Graphics, Imaging, and Vision, CGIV 2010* (IS&T, Springfield, VA, 2010), pp. 504–509.